Quantification of Macro- and Micro-vascular Hemodynamics in Cerebral Arteriovenous Malformations during Staged Embolization

Can Wu[1], Timothy Carroll[1], Parmede Vakil[1], Sameer Ansari[2], Bernard Bendok[2], Hunt Batjer[3], and Michael Markl[1]

[1]*Departments of Biomedical Engineering and Radiology, Northwestern University, Chicago, IL, United States,* [2]*Departments of Radiology and Neurological Surgery, Northwestern University, Chicago, IL, United States,* [3]*Department of Neurological Surgery, UT Southwestern, Dallas, TX, United States*

Introduction: Cerebral arteriovenous malformations (AVMs) are abnormal direct connections between arteries and veins without an intervening capillary bed. They account for about 2% of all hemorrhagic strokes each year [1]. Digital subtraction angiography (DSA) combined with selective intra-arterial iodine contrast injections guides AVM treatment by staged embolization procedures, often followed by surgical resection or radiosurgery after shrinkage of the AVM nidus. However, it is often unclear which feeding artery should be targeted for embolization and how this will affect hemodynamic outcome. In addition, it is unclear how AVMs and their treatment affect microvascular perfusion and thus perinidal ischemia due to steal effects potentially associated with large and high-flow AVMs. DSA provides excellent AVM vascular imaging but is highly invasive and includes substantial exposure to ionizing radiation. Non-invasive monitoring of embolization induced changes has been limited by the lack of modalities to quantitatively assess AVM hemodynamics and microvascular perfusion of the surrounding brain tissue. To address this limitation, we applied a comprehensive MRI and analysis protocol for quantitative characterization of 3D AVM hemodynamics and brain tissue perfusion with 4D flow and perfusion MRI [2, 3].

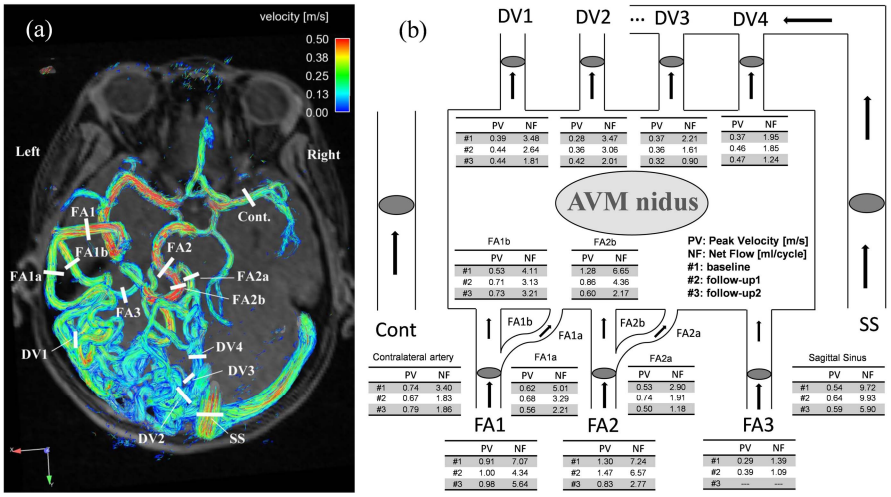

Fig.1: 3D paticle traces of the AVM-4 vasculature with vessle labels at baseline (a); schematic AVM model and quantification of the peak velocities (PV in m/s) and net flow (NF in ml/cycle) in major feeding arteries (FA), draining veins (DV), sagittal sinus (SS), and conralateral arteries (Cont) at baseline (#1) and follow-up scans (#2, #3) during embolization (b).

Methods: 4 AVM patients (age=33±10 years, 1 female, SMG=3 (n=3), SMG=4 (n=1)) were included in our study. Baseline and follow-up MRI after interventional treatment by staged embolization was performed in all 4 patients on 1.5T or 3T MR systems (Siemens, Germany). ECG-gated 4D flow (VENC=1m/s, flip angle=15°) with full coverage of the AVMs was acquired for 3D visualization and quantification of AVM blood flow characteristics (EnSight, CEI, USA). Gd-DTPA contrast agent (Magnevist, NJ, USA) was injected for perfusion MRI scans (spin-echo SCALE-PWI [3], flip angle=20°). AVM hemodynamics was visualized using time-integrated 3D pathlines depicting the AVM arterial feeding and venous draining patterns over the cardiac cycle (Fig. 1a). Schematic AVM models (Fig. 1b, example for AVM-4) were built for AVMs including the major feeding arteries (FA), draining veins (DV), sagittal sinus (SS) and contralateral arteries. Peak velocity (PV in m/s) and net flow (NF in ml/cycle) were calculated for all vessels. Perfusion markers (CBF, CBV, and MTT) in the ipsilateral and contralateral regions of interest (ROIs, Fig. 3) were quantified to evaluate the impact of embolization on systemic changes in microvascular tissue perfusion. Spatial co-registration of the 4D flow data (particle traces) and perfusion images was performed to provide a joint visualization of macrovascular 3D blood flow and microvascular tissue perfusion (Fig. 3).

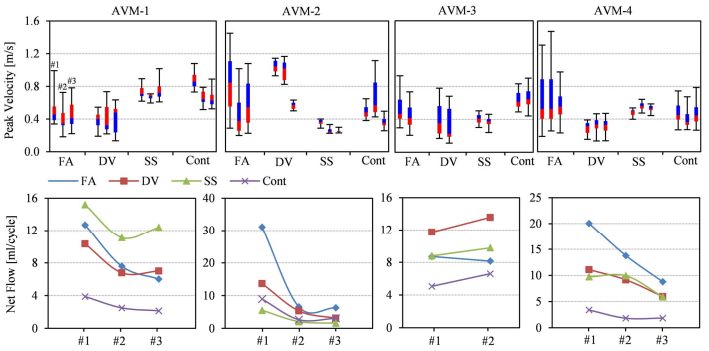

Fig. 2: Large vessel quantification of 4 AVM patients (baseline #1, follow-ups #2, #3; AVM-3 only has one follow-up #2). PV: peak velocity distribution with box plots; NF in FA (DV): sum of the NF in all arterial feeders (draining veins).

Results: 3D blood flow visualization of AVM-4 at baseline and its corresponding AVM model with quantified PV and NF in each vessel are shown in Fig. 1. For this patient, 3 major feeders (FA1-FA3) and 4 draining veins (DV1-DV4) were identified. FA1 and FA2 had additional bifurcations. Note that FA3 was completely occluded during follow-up2 (#3). DV3 and DV4 drained directly into the sagittal sinus. Similar models were built for other 3 AVMs (AVM-1: FA (n=5), DV (n=4); AVM-2: FA (n=4), DV (n=1); AVM-3: FA (n=3), DV (n=3)). Fig. 2 illustrates changes of PV and NF for all 4 patients from baseline to follow-up scans. Distinct changes of the distribution of PV and NF across arterial feeders can be observed in all vessels, but the alterations are highly patient specific. Spatial co-registration of the CBF images (color coded, example for slice #8) and particle traces (gray scale) was performed for 3 AVM patients at baseline (Fig. 3). High CBF (red) and high blood flow velocity (white) were observed within each AVM nidus. During follow-up, the CBF ratios of ROI-A (contralateral) to ROI-B (ipsilateral) were decreased indicating a relative increase of blood flow to the ipsilateral tissue after embolization (Fig. 3).

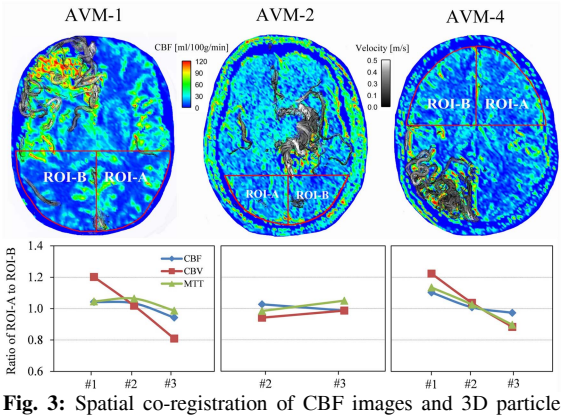

Fig. 3: Spatial co-registration of CBF images and 3D particle traces for 3 patients at baseline and contralateral (ROI-A) to ipsilateral (ROI-B) tissue perfusion ratios during embolization. Perfusion data of AVM-2 at baseline (#1) was removed due to contrast agent injection failure.

Discussion: 4D flow and perfusion MRI were successfully employed to provide quantitative information on both macro- and micro-vascular hemodynamics in AVM patients. Changes in arterial feeding and venous draining patterns as well as perinidal tissue perfusion demonstrated the ability to assess complex hemodynamic changes for the individual AVM patient. Combined 4D flow and brain tissue perfusion MRI may thus be useful for pre-treatment planning and post-treatment evaluation. However, higher spatial resolution is required to depict small vascular structures since only the large feeding arteries and draining veins were identified in our study.

Acknowledgements: Grant support by NIH/NIBIB T32 EB005170.

References: [1] Khan SU, et al. *MMJ*, 19:438-441, 2010. [2] Markl M, et al. *JCMR*, 13:7, 2011. [3] Srour JM, et al. *JCBFM*, 31:1272-1282, 2011.